[1.]Arun KUMAR, [2.]Sandeep Singh SANDHU, [3.]Beant SINGH

CHARACTERIZATION OF MECHANICAL PROPERTIES AND MICROSTRUCTURE OF ELECTRON BEAM WELDED AISI 316 STAINLESS STEEL

[1&2.]Department of Mechanical Engineering, Quest Infosys Foundation Group of Institutions, Jhanjeri Mohali (Punjab), INDIA
[3.]Department of Mechanical Engineering, Punjab College of Engineering and Technology, Lalru, Punjab, INDIA

Abstract: A defect free, full penetrated welded joint of 18mm thick AISI 316 was obtained in a single pass by optimized welding parameters of electron beam welding. Owing to the rapid solidification behavior (from FA to AF) associated with the electron beam welding different microstructural morphology was observed. Microstructure obtained by optical microscope revealed the skeletal and columnar dendritic ferrite in weld metal. The tensile strength and impact toughness of the weld zone was observed lower than the base metal. Further, after thermal aging at 750°C for 24 hours and 300 hours the precipitation of carbides were observed in welded joints, which affected the mechanical properties. The impact toughness showed 50%reduction after thermal aging, whereas tensile properties showed negligible change. The microhardness of the welded joint increased after thermal aging from all the regions with maximum value at HAZ.
Keywords: Electron beam welding, thermal aging, microstructure, mechanical properties, AISI 316 austenitic stainless steel

1. INTRODUCTION

Electron beam welding (EBW) is a fusion welding process used to weld the different grades of steel, refractory metals, chemically active metals and various non-metals. This is a keyhole welding technique used to weld steel with thickness varied from 0.01 mm to 250 mm and aluminum up to 500 mm [1]. The exceptional qualities of EBW is its capability to weld with high depth to width ratio, narrow weld zone and HAZ, low distortion, greater productivity and absence of secondary phases and residual stress[2]–[4]. However, the need of vacuum environment is restricted its application in large assemblies parts. Owing to the advantages of the EBW, it is best suited for welding thick section austenitic stainless steel used in nuclear, power generation, food, textile, oil and many other industries [5]–[7].

The other welding processes used to weld for thick section of austenitic stainless steel are shielded metal arc welding and tungsten inert gas welding [8]. These processes are very slow, requires many passes and induced high heat input, results in coarse grains structure, wider heat affected zone (HAZ), high distortion and poor productivity [7]. Many researchers used electron beam welding for the welding of thick plate stainless steels. Xia et al. [9] obtained 4mm width of weld zone in 50mm butt joint of AISI 316L with electron beam welding and found that the mechanical properties are under considerable range.

Alali et al. [8] welded 20 mm thick austenitic stainless steel with EBW and analyzed that microstructure consists of columnar and dendritic ferrite. Authors concluded that the ultimate tensile strength is higher at bottom of the weld zone than top region, whereas hardness at base metal and HAZ zone is higher than weld zone.

Tjong et al. [10] performed microstructural characteristics analysis of AISI 316L welded with electron beam welding. The microstructure study showed that high cooling and under cooling associated with electron beam caused formation of cellular and equiaxed dendrites. The hardness was higher in HAZ and weld metals than the base metal.

ANNALS of Faculty Engineering Hunedoara – International Journal of Engineering
ISSN 1584 - 2665 (printed version); ISSN 2601 - 2332 (online); ISSN-L 1584 - 2665
Universitatea Politehnica Timişoara

The presence of high carbon content in austenitic stainless steel increases the harmful carbide precipitation during welding and high temperature applications. This affects the mechanical properties and corrosion resistance of the weld joint, results in the failure of component from weld region [11]. The EBW reduces the precipitation of carbides as compare to the convention welding processes because it induced low heat input in welded joint. Zumelzu et al. [12] analyzed that the thermal contribution was directly effects the tensile properties and ferrite content of AISI 316L welded joints. Kim et al. [13]concluded that the thermal aging of 316 SS at 650°C and 750°C for 10 hours reduced the mechanical properties whereas the aging at 600°C for 10 hours reduced the tensile properties marginally. Kozuh et al. [14] concluded that after post weld heat treatment the impact toughness and hardness decreases from base metal and HAZ.

In the present work, electron beam welding of 18mm thick AISI 316 stainless steel has been carries out. Square butt welds were subjected to metallurgical and mechanical properties analysis. To investigate the effect of carbides precipitation on the mechanical and metallurgical properties, specimens were subjected to thermal aging at 750°C for 24 hours and 300 hours.

2. MATERIALS AND METHODS

AISI 316 austenitic stainless steel plates of 18 mm thickness with 75mm width and 150 mm length were used for this study. The chemical composition of the base metal is shown in table 1.

Table 1: Chemical composition of AISI 316 weight %

Element	C	Cr	Ni	Mo	Si	Mn	S	P	Fe
Weight %	0.064	16.15	10.44	2.18	0.54	0.95	0.025	0.023	Balance

The plates were welded with electron beam welding without using any filler metal and by considering beam voltage 150 kV and beam current 90 mA as major parameters. The vacuum during welding was $5x10^{-6}$ mbar. Trail experiments were conducted to achieve the full penetration and defect free joint in a single pass. The full penetration was achieved at welding speed of 700 mm/minute. The heat input by considering the 95% efficiency of the welding process was 1.10kJ/mm. Before welding, the plates were machined precisely to narrow square butt joint and clean chemically to remove dust, grease and other elements. Further to analyze the effect of carbides precipitations on the welded joints, two thermal ageing processes were performed on the extracted specimens viz. thermal aging at 750°Cfor 24 hours and thermal aging at 750°C for 300 hours.

3. RESULTS AND DISCUSSIONS

AISI 316 stainless steel 18mm thick welded joint was fabricated by electron beam welding. The welded joint was subjected to ultrasonic scan test to analyze the weld defect. The weld was free from any defects and was subjected to various tests viz. tensile test, impact toughness test, mircohardness and microstructure analysis. The separate tests were conducted for as-welded specimens and thermally aged specimens.

—Tensile tests

The tensile test samples were extracted as per ASTM E8 standard from the welded joint[15]. The tensile tests were performed on Tinius Olsen tensile testing machine of 50 kN capacity with displacement rate of 2mm/min. All the samples were broken from the center of the weld zone, which showed that the welded joint was weaker than the base metal. Figure 1 showed the tensile specimens fractured at the weld zone after tensile testing.

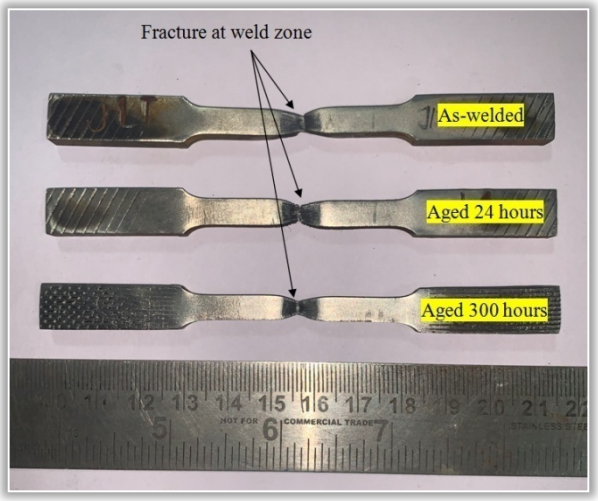

Figure 1: Tensile specimens fractured from weld zone

The UTS in as-welded condition was recorded 559 MPa which is less than UTS of base metal (571 MPa). After thermal aging at 750°C for 24 hours, UTS increased by 4% and percentage elongation increased by 7% whereas, 300 hours aged specimens showed decrease in UTS and % elongation. Further, the continuous reduction in YS was recorded after thermal aging processes. This reduction in tensile properties after thermal aging may attribute to the formation of the carbides. Figure 2 showed the UTS, percentage elongation and YS of specimens in as-welded condition and after thermal aging processes.

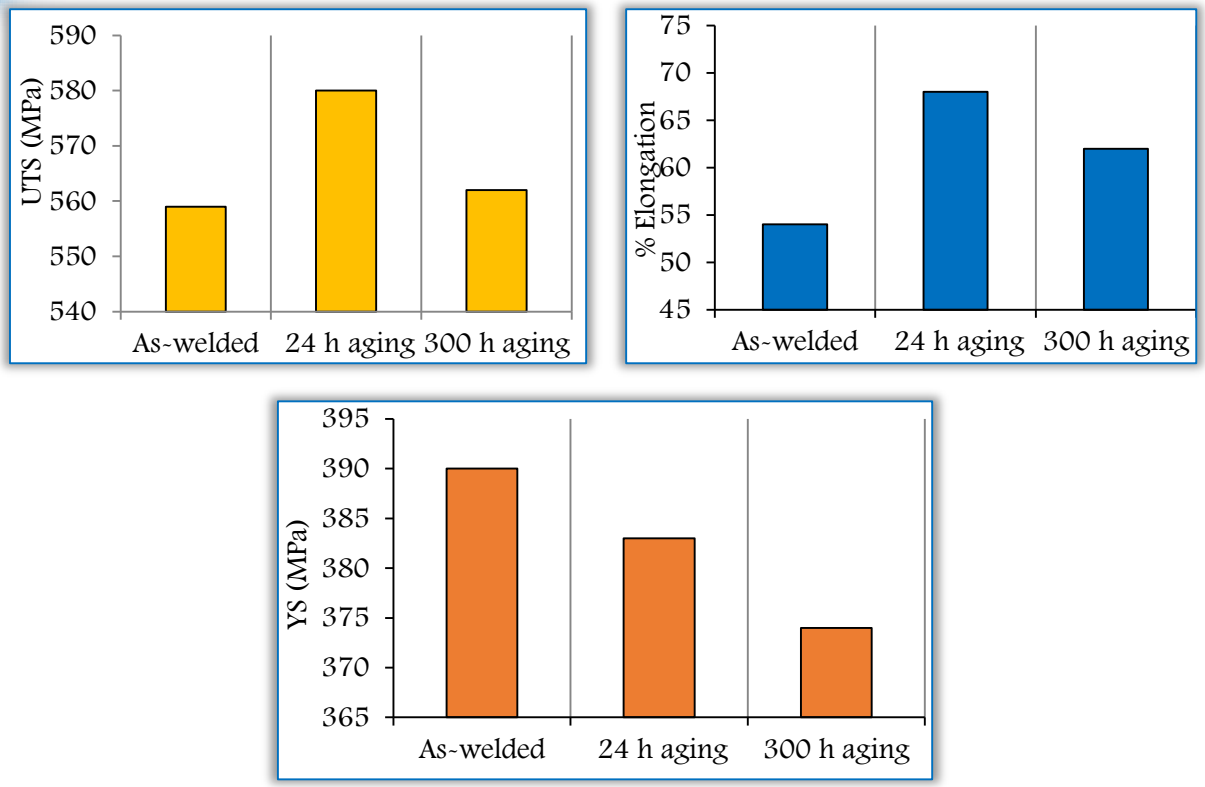

Figure 2: UTS, % Elongation and YS of EB welded joints

—Charpy V-notch impact tests

The electron beam welded specimens were subjected to Charpy V-notch impact test at sub-zero (-20°C) temperature. The specimens were extracted as per ASTM E 23 standard with dimension 55 x 10 x 10 mm[16]. The v-notch at 45° with 2mm depth was machined at the center of weld zone with direction perpendicular to the depth of the weld. Figure 3 showed the broken specimens after Charpy V notch impact test.

Figure 3: Specimens after Charpy V-notch impact tests

The results of the impact toughness are plotted in figure 4. In maximum average impact energy of 144.3 J was absorbed by as-welded specimen. The energy absorbed was reduced after thermal aging processes, the average impact toughness recorded in specimen aged at 750°C for 24 hours was 72.5J and specimen aged at 750°C for 24 hours was 59.7J. The impact toughness test results clearly indicated that the carbides formation after the thermal aging processes reduced the ductility of the welded joint.

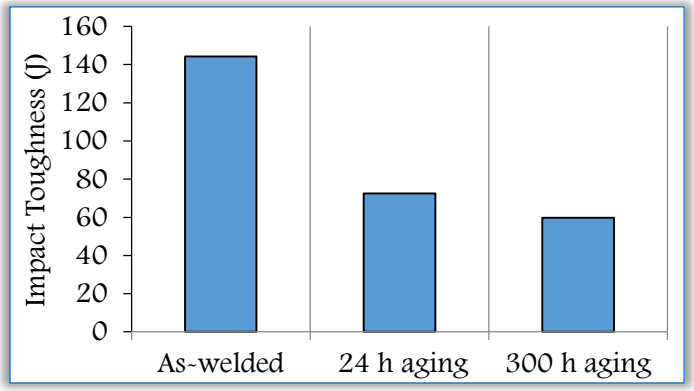

Figure 4: Impact toughness of welded joints at sub-zero temperature

— Microhardness properties

Figure 5 shows the result of microhardness at weld zone, HAZ and base metal in as-welded condition and after thermal aging processes. The Vickers microhardness test was conduction across the weld bead by using load of 1000 gm with dwell time of 30 sec. The maximum microhardness was recorded at HAZ in all the specimens. The specimen aged at 750°C for 300 hours showed higher mircohardness in all regions. This may attribute the carbides precipitation, which transforms the ferrite content into secondary phases. The microhardness results wereassociated with the results of impact toughness. Dinda et al. [2] reported the maximum microhardness at HAZ of the welded joint. Komerla et al. [17]also showed the increase in microhardness after thermal aging process.

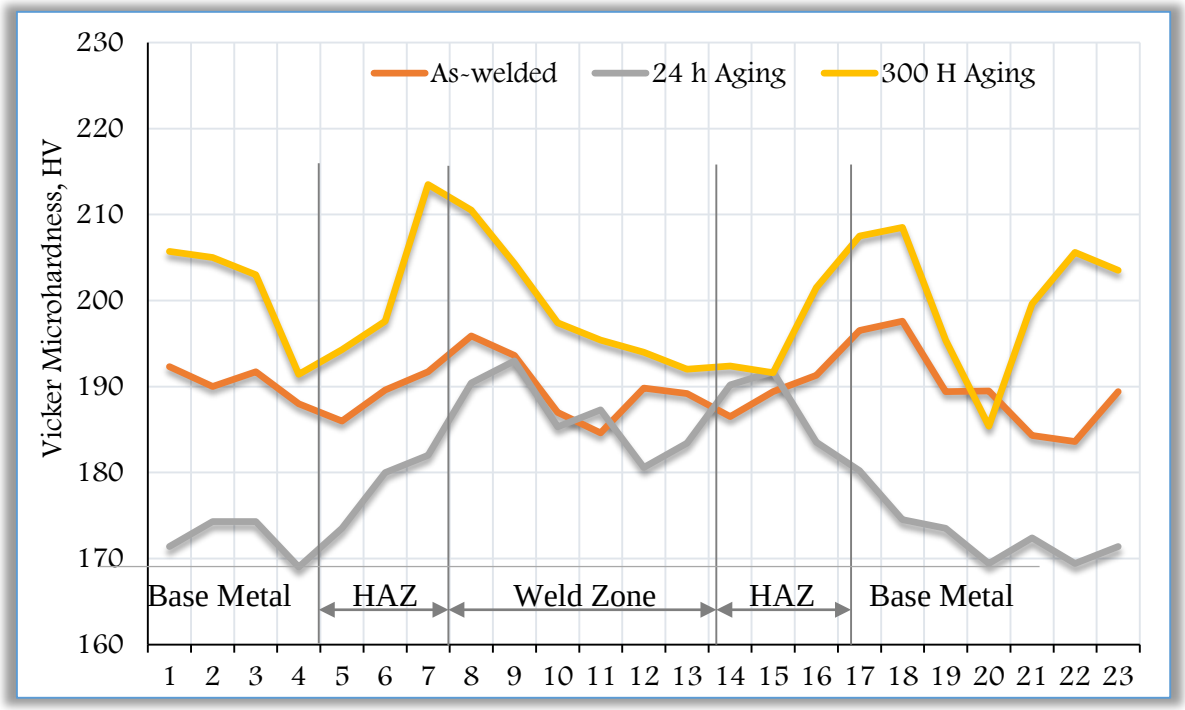

Figure 5: Mircohardness across the weld bead

— Microstructure analysis

To reveal the microstructure, the metallographic specimens were carefully polished by silicon carbide papers and etched with aqua regia etchant. The microstructure of the welded joint was analyzed by optical microscope. Figures 6, 7 and 8 represent the microstructure of the welds in as-welded condition, after thermally aged at 750°C for 24 hours and 300 hours respectively. The weld zone of as-welded specimen consists of columnar dendritic and skeletal ferrite structure, as shown in figures 6a and 6b. This non-uniform structure of the weld zone may attribute to the rapid cooling associated with low heat input welding [18]. The figure 6c depicts that the direction of the formation of skeletal ferrite is perpendicular to the center of the weld. The parting line is visible at the center of the weld. All the tensile specimens were fractured from this parting line.

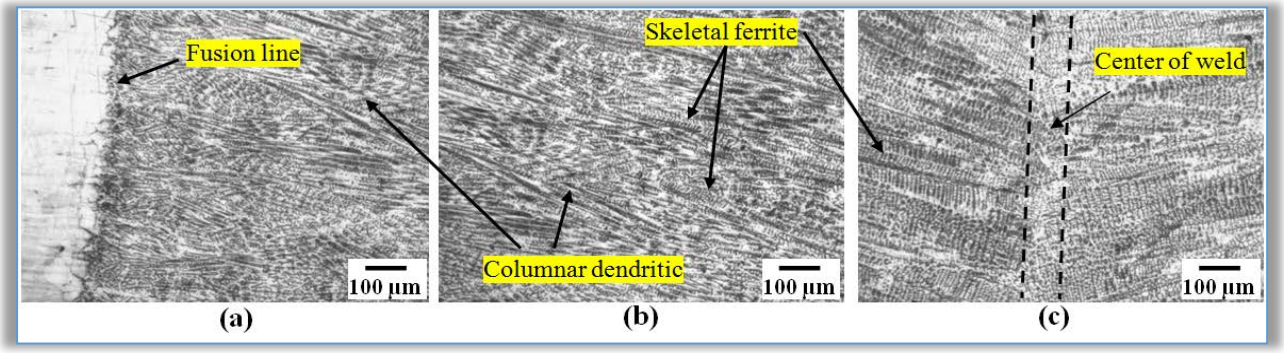

Figure 6: Microstructure in as-welded condition (a) fusion line, (b) weld zone and (c) Center line.

Figure 7 shows the precipitation of the carbides in the weld zone after thermal aging at 750°C for 24 hours. The ferrite dendrites were not fully transformed into carbides as traces of skeletal ferrite

was reveled in the structure, as shown in figures 7a and 7b. Figure 8 represents the carbides precipitation after the thermal aging at 750°C for 300 hours. By comparing figure 8 with figure 7, it was clear that the density of carbides increased after aging for 300 hours. Figure 8a shows the precipitation of carbides in base metal and near fusion line. Figures 8b and 8c also show the dense precipitation of carbides, depicts the decomposition of the ferrite content in the weld zone. Further, the results of the microstructure analysis were found to be in association with the impact toughness results and microhardness results.

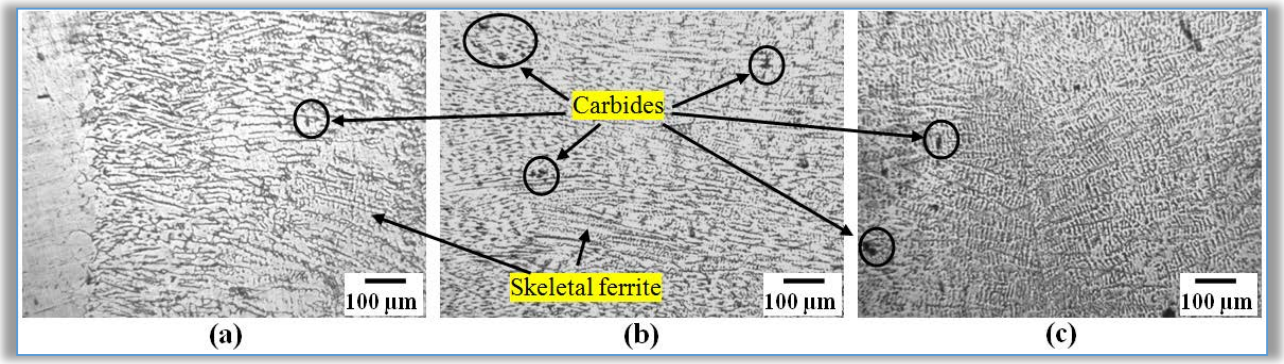

Figure 7: Microstructure after thermal aging at 750°C for 24 hours (a) fusion line, (b) weld zone and (c) Center line

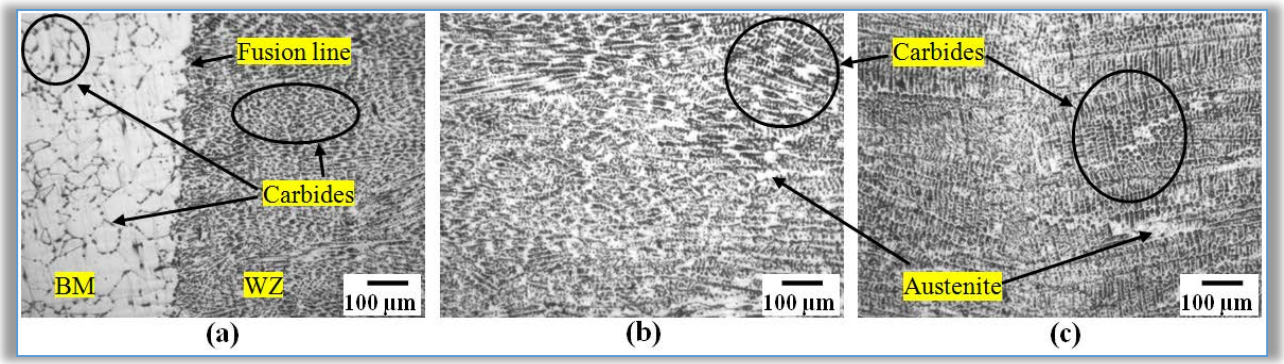

Figure 8: Microstructure after thermal aging at 750°C for 300 hours (a) fusion line, (b) weld zone and (c) Center line

4. CONCLUSIONS

To characterize the electron beam welds of AISI 316 stainless steel, the mechanical and microstructural properties in as-welded condition and after thermal aging processes were investigated. On the basic of results mentioned in section 3, following conclusions could be drawn.

- Defect free, fully penetrated 18 mm thick plate was fabricated successfully with electron beam welding in a single pass.
- The tensile strength results show that the welded joints were weaker that the base metal, although the tensile strength of welded joints were under considerable limit. After thermal aging there was marginally change in UTS and YS but change in ductility was considerable.
- The Charpy impact test results shows that after thermal aging for 24 hours the impact toughness reduced by approximately 50%. After thermal aging for 300 hours, 58% reduction in impact energy was reported.
- The microstructure analysis revealed the skeletal and columnar ferrite in as-welded specimens, whereas carbides were precipitated after thermal aging.
- The impact toughness, microhardness and ductility of the welded joints were in association with microstructure.

ACKNOWLEDGEMENTS

We wish to acknowledge the Mechanical Engineering Department, IKGPTU Kapurthala, SLIET Longowal, PEC Chandigarh and IIT Ropar for their testing facilities.

References

[1] A. Klimpel, Welding Handbook, Vol 1. Silesian University of Technology, Gliwice, 2013.
[2] S. K. Dinda, M. Basiruddin Sk, G. G. Roy, and P. Srirangam, "Microstructure and mechanical properties of electron beam welded dissimilar steel to Fe–Al alloy joints," Materials Science and Engineering A,

2016, doi: 10.1016/j.msea.2016.09.050.
[3] T. Wang, Y. Zhang, X. Li, B. Zhang, and J. Feng, "Influence of beam current on microstructures and mechanical properties of electron beam welding-brazed aluminum-steel joints with an Al5Si filler wire," 2017, doi: 10.1016/j.vacuum.2017.04.029.
[4] S. Guo et al., "Effect of beam offset on the characteristics of copper/304stainless steel electron beam welding," Vacuum, 2016, doi: 10.1016/j.vacuum.2016.03.034.
[5] K. Weman, "Introduction to welding," Welding Processes Handbook, pp. 1–12, 2013, doi: 10.1533/9780857095183.1.
[6] S. Goyal, S. Mandal, P. Parameswaran, R. Sandhya, C. N. Athreya, and K. Laha, "A comparative assessment of fatigue deformation behavior of 316 LN SS at ambient and high temperature," Materials Science and Engineering: A, vol. 696, pp. 407–415, 2017, doi: 10.1016/j.msea.2017.04.102.
[7] X. Zhang et al., "Welding of thick stainless steel plates up to 50 mm with high brightness lasers," Journal of Laser Applications, vol. 23, no. 2, p. 022002, 2011, doi: 10.2351/1.3567961.
[8] M. Alali, I. Todd, and B. P. Wynne, "Through-thickness microstructure and mechanical properties of electron beam welded 20 mm thick AISI 316L austenitic stainless steel," Materials & Design, 2017, doi: 10.1016/j.matdes.2017.05.080.
[9] X. Xia et al., "Correlation between microstructure evolution and mechanical properties of 50 mm 316L electron beam welds,"Fusion Engineering and Design, vol. 147, no. June, p. 111245, 2019, doi: 10.1016/j.fusengdes.2019.111245.
[10] S. C. Tjong, S. M. Zhu, N. J. Ho, and J. S. Ku, "Microstructural characteristics and creep rupture behavior of electron beam and laser welded AISI 316L stainless steel," vol. 227, pp. 24–31, 1995.
[11] J. Kar, S. K. Roy, and G. G. Roy, "Effect of beam oscillation on electron beam welding of copper with AISI-304 stainless steel," Journal of Materials Processing Technology, 2016, doi: 10.1016/j.jmatprotec.2016.03.001.
[12] E. Zumelzu, J. Sepúlveda, M. Ibarra, and J. Sepu, "Influence of microstructure on the mechanical behaviour of welded 316 L SS joints," Journal of Materials Processing Technology, vol. 94, no. 1, pp. 36–40, 1999, doi: 10.1016/S0924-0136(98)00450-6.
[13] H. S. Kim et al., "Effects of heat treatment on mechanical properties and sensitization behavior of materials in dissimilar metal weld," International Journal of Pressure Vessels and Piping, vol. 172, no. March, pp. 17–27, 2019, doi: 10.1016/j.ijpvp.2019.03.009.
[14] S. Kozuh, M. Gojic, and Kose, "Mechanical properties and microstructure of austenitic stainless steel after welding and post-weld heat treatment," Kovové Materiály, vol. 47, no. 4, pp. 253–262, 2009.
[15] ASTM E8, "ASTM E8/E8M standard test methods for tension testing of metallic materials 1," Annual Book of ASTM Standards 4, no. C, pp. 1–27, 2010, doi: 10.1520/E0008.
[16] ASTM E23-12c, "Standard Test Methods for Notched Bar Impact Testing of Metallic Materials," vol. i, 2013, doi: 10.1520/E0023-12C.2.
[17] K. Komerla et al., "The effect of beam oscillations on the microstructure and mechanical properties of electron beam welded steel joints," International Journal of Advanced Manufacturing Technology, vol. 102, no. 9–12, pp. 2919–2931, 2019, doi: 10.1007/s00170-019-03355-4.
[18] M. Zhang, G. Chen, Y. Zhou, and S. Liao, "Optimization of deep penetration laser welding of thick stainless steel with a 10kW fiber laser," Materials and Design, vol. 53, pp. 568–576, 2014, doi: 10.1016/j.matdes.2013.06.066.

ANNALS of Faculty Engineering Hunedoara – International Journal of Engineering
ISSN 1584 - 2665 (printed version); ISSN 2601 - 2332 (online); ISSN-L 1584 - 2665